

## Research Article

# Bridged Phthalocyanine Systems for Sensitization of Nanocrystalline TiO<sub>2</sub> Films

**Gloria Zanotti,<sup>1</sup> Nicola Angelini,<sup>2</sup> Sara Notarantonio,<sup>2</sup> Anna Maria Paoletti,<sup>2</sup> Giovanna Pennesi,<sup>2</sup> Gentilina Rossi,<sup>2</sup> Angelo Lembo,<sup>1</sup> Daniele Colonna,<sup>1</sup> Aldo Di Carlo,<sup>1</sup> Andrea Reale,<sup>1</sup> Thomas M. Brown,<sup>1</sup> and Giuseppe Calogero<sup>3</sup>**

<sup>1</sup> Center for Hybrid and Organic Solar Energy (CHOSE), University of Rome "Tor Vergata", Via Giacomo Peroni 400/402, 00131 Rome, Italy

<sup>2</sup> CNR-Istituto Struttura della Materia, Via Salaria Km. 29.5, Monterotondo Stazione, 00016 Rome, Italy

<sup>3</sup> CNR, Istituto per i Processi Chimico-Fisici, Salita Sperone Contrada Papardo, Faro Superiore, 98158 Messina, Italy

Correspondence should be addressed to Gentilina Rossi, gentilina.rossi@ism.cnr.it

Received 1 June 2010; Accepted 28 June 2010

Academic Editor: Leonardo Palmisano

Copyright © 2010 Gloria Zanotti et al. This is an open access article distributed under the Creative Commons Attribution License, which permits unrestricted use, distribution, and reproduction in any medium, provided the original work is properly cited.

Phthalocyanines based-dyes represent attractive alternatives to the expensive and polluting pyridyl based Ru complexes because of their photochemical and thermal stability, they do show in fact intense absorption in the UV/blue (Soret band) and the red/near IR (Q band) spectral regions and appear very promising as sensitizer dyes for DSSC. In this contribution we review the state of the art and the recent progress in the application of these materials as dyes for DSSC and present three new dyes which are bridged derivatives of Iron phthalocyanine. Synthesis, optical properties, electrochemical characterization and device performances are discussed with regard to the different substitution degree of the macrocycle.

## 1. Introduction

The achievement of an efficient conversion of sun light into electricity is a compelling scientific target considering the worldwide increasing demand for energy and the fact that the sunlight is certainly the largest and available single source of clean energy. Although several new technologies have been developed for this purpose they are not yet an economically viable alternative to fossil fuels [1]. Among organic photovoltaic (OPV) family, Dye Sensitized Solar Cells (DSSC) exhibit a conversion efficiency value lower than the corresponding photovoltaic devices based on silicon [2]. Nevertheless they represent, nowadays, a solid alternative for less-expensive photovoltaic energy production attracting the commercial interest of many industrial companies such as Aisin Seiki, Konarka, Dyesol, and G24 innovations, Limited.

In a schematic way the assembly of a typical DSSC is realised by a mesoporous TiO<sub>2</sub> film (photoanode), with a charge transfer dye anchored on the surface, placed in contact with a solid state hole-conductor film (shuttle

and a photoinert counter electrode (cathode) [3]. In the most studied and efficient devices to date, light is adsorbed by a polypyridyl ruthenium-based complex (dye) that is linked to titanium oxide surface via carboxylate moieties; the photoanode is a thick (~12 μm) film of TiO<sub>2</sub> nanoparticles (10–20 nm), yielding a conversion efficiency ( $\eta$ ) up to 10%–11% and stable operation for millions of turnovers. The photoexcitation of the Ru-complex results in an intramolecular metal-to-ligand charge-transfer (MLCT) transition and the photoexcited electrons located on the bipyridyl ligands can be efficiently injected into the conduction band of the TiO<sub>2</sub> on an ultrafast time scale via carboxyl group anchored to the TiO<sub>2</sub> surface [4]. A large electronic coupling between the photosensitizer and the conduction band is exhibited by this combination. Conversely, the recombination between the injected electrons and the dye cation is a slow process [5] and it is considered to be a result of the large separation between the TiO<sub>2</sub> and the Ru<sup>3+</sup> due to the bipyridyl ligands. Developing new effective organic dye sensitizers with good light-harvesting features is a current challenge

for many research groups as the polypyridyl-type complexes of ruthenium, successfully employed, show some significant restrictions as the low optical absorbance in the red/near infrared spectral regions as well as a low molar extinction coefficient and a nonenvironmental friendly production of the ruthenium. As it is believed that the simultaneous development of new dyes, shuttles, and photoanodes will lead to DSSCs with efficiencies exceeding 16% [6], the extensive research efforts targeting new sensitising molecules as alternative candidates suitable to overcome at least some of these limits appear to be more than justified. A large number of new organic dyes have been developed during these last few years, several research groups have developed metal-free organic sensitizers and obtained efficiencies in the range of 4%–8% [7]. The major advantages of these metal-free dyes are their tunable absorption and electrochemical properties through suitable molecular design [8]. Remarkable results was reported by Tian et al. [9] and Hagberg et al. [10] with novel metal-free dyes that showed a broader incident photon-to-current conversion efficiency spectrum over the whole visible range extending into the near-IR region up to 920 nm; in one case they reached the conversion efficiency of 7.20% under standard AM 1.5 sun light. Among dyes that address both spectral coverage and absorptive issue are included indolines [11]; a significant improvement in the cell performances was also made by the group of Hara et al. [12, 13], using coumarin or polyene type sensitizers, achieving solar to electric power conversion efficiencies reaching up to 7.7% in full sunlight. Natural pigments containing anthocyanins and carotenoids, although have shown overall solar energy conversion efficiencies around 1%, are also currently investigated [14]. Both porphyrins (Ph) and phthalocyanines (Pc) represent a class of dyes considered attractive alternatives to the expensive and polluting pyridyl-based Ru complexes, the former because of the analogy with natural photosynthetic molecules the latter because of their photochemical and thermal stability [15]. However porphyrins cannot compete with Ru-complexes due to their lack of red light and near IR absorption while phthalocyanines seem more promising because of their intense absorption in the UV/blue and the red/near IR spectral regions and because of the flexibility in modulating the spectroscopic features and tuning the electrochemical properties.

In this contribution we extensively review the state of art on these specific dyes, pointing out the most relevant achieved results in terms of efficiency of the related DSSCs and key points still to be improved. Furthermore, the synthesis strategy and preliminary data on new dyes based on phthalocyanine bridged systems as building blocks for highly conjugated superchromophores will be presented.

## 2. Phthalocyanine-Based Dyes for DSSCs: State of Art

Phthalocyanines and their metalloderivatives are a very well-known class of materials for their industrial applications as green and blue dyestuffs, but more recently renewed and growing interest, due to their outstanding chemical

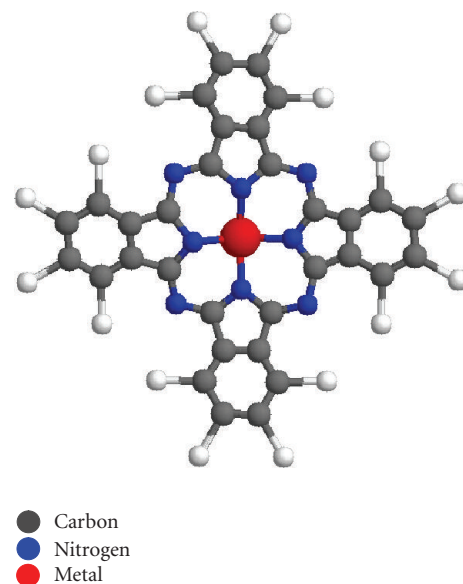


FIGURE 1: General structure of a metal phthalocyanine.

and physical properties, has been involving many research groups, and different fields of science and technology are currently investigated. They include, among others, chemical sensors, electrochromic display devices, molecular metals and conducting polymers, photodynamic cancer therapy, liquid crystal, catalysts, and photovoltaic cell elements, with both fundamental and applied aspects continuously explored [16]. In Figure 1 the metal phthalocyanine molecule is sketched and some fundamental features can be pointed up; it is a strictly planar molecule with high charge delocalisation ( $18\pi$  electrons), high thermal stability, easy processability, low solubility in the most conventional organic solvents, and intense colour (blue, green, purple). It also exhibits linear and nonlinear optical properties, magnetic properties (depending on the central metal), electrochemical (electrochromic displays), and electrical (semiconductor, photoconductor) features. Next to their unusual chemical and physical characteristics a further advantage is offered by the tailoring of these properties; for instance, the introduction of bulky groups or alkyl chains in the peripheral ring enhances the solubility as well as influences their electronic configurations. Furthermore, metal phthalocyanines can be also combined as building blocks with other organic molecules to assemble new molecular aggregates of interest in electronics and optoelectronics [17].

In this contribution we want to limit our update to the exploit of metal phthalocyanines and its derivatives in the construction of solar cells (DSSC), and to underline that in spite of the fact that phthalocyanine-based cells still do not reach efficiencies as good as Ru-based cells, they are as well considered “appealing materials” for photoconversion process because of their already described features [18]. Indeed a DSSC device is a sophisticated multicomponents system not yet understood in detail; certainly the optimisation of all the constituents of the device would participate in determining

the final performance even if the dye, together with other elements, is a key factor because of its light harvesting function [19]. A single dye normally does not absorb all the photons from the visible and near-infrared region, so the research for innovative approaches that increase the number of active sites on the semiconductor surface and the charge collection efficiencies is a significant issue that has been originally faced from the study by Hardin et al. in [20] exploiting the Forster resonant energy process obtained adding a highly luminescent chromophores inside the liquid electrolyte, and from the study by Lee et al. in [21], developing an original method to get a selective positioning of organic dyes on the surface of the TiO<sub>2</sub> semiconductor. Basically, the theoretical requirements for a good dye are numerous [22]: (1) it should be strongly attached to the semiconductor surface, (2) it should exhibit absorption in the whole solar spectrum, (3) its LUMO (Lowest Unoccupied Molecular Orbital) should present a higher energy than the conduction band (CB) edge of the semiconductor and good orbital overlap to facilitate electron injection, (4) charge recombination between the injected electron and the oxidized dye should be slow enough for the electron transport to the external circuit, (5) its redox potential should be more positive than the one of the redox couple in the electrolyte so that it can be quickly regenerated, (6) it should be stable for long-time exposure to natural sunlight, and (7) it should be soluble in a solvent compatible with the semiconductor and favourable for adsorption of nonaggregated monolayer on the surface. It is obviously difficult to design a dye fulfilling all the requisites and, with regard to those owned by phthalocyanine derivatives, it can be highlighted that they do show intense absorption in the Uv/blue (Soret band) and in the red/near IR (Q band) spectral region, and they are also transparent over a large region of the visible spectrum, offering the possibility of using them as “photovoltaic windows”. Phthalocyanines can be anchored to the TiO<sub>2</sub> semiconductor surface in two different ways allowing to dispose the molecules in a parallel arrangement (anchoring group in the axial position) [23–25] or in a more or less perpendicular orientation (anchoring group inserted in the peripheral macrocycle) [26]. Their applications in DSSCs have been limited up to date for two essential reasons: the first one is associated with the aggregation phenomena of the macrocycles on the semiconductor surface, resulting in a rapid deactivation of the dye’s excited state; the second one is due to the LUMO level position considered too low and lacking of the appropriate directionality for the electron transfer into the TiO<sub>2</sub> conduction band; this latter, being a key point for efficient overlapping between the molecular orbitals and the semiconductor CB, is an aspect to be considered in designing new phthalocyanine-based dyes.

In order to exceed the first limitation, sterically hindered phthalocyanines bearing peripheral phenyl groups have been synthesized by Eu et al. [27] and, in the presence of a high degree of substitutions, suppressed aggregation phenomena have been shown. The incorporation of tyrosine groups into zinc phthalocyanine molecule reduces, as well, the surface aggregation which can always be assigned to steric

hindrance [22]. However the introduction of bulky groups produces a low improvement in device performance; better results have been achieved when small organic acids have been contextually added [28]. In a recent paper [29] the influence of coadsorbents upon interfacial electron transfer has been deeply investigated. The authors prove, in a detailed study, that the addition of two additives as Li<sup>+</sup> and chenodeoxycholic acid (CHENO) in a series of novel ruthenium phthalocyanines produces a considerable effect on the electron transfer dynamics; the influence of the two coadsorbents on the electron injection into the semiconductor CB, on the recombination of the oxidized dye with the electrons in TiO<sub>2</sub>, and on the regeneration of the oxidized dye by the redox electrolyte are thoroughly discussed. The results show that the justification for the enhanced photocurrent is not the suppression of dye aggregates but the slower recombination of dye cations with the TiO<sub>2</sub> electrons and the faster regeneration of the dye cations by the electrolyte.

The use of an axial ligation besides lowering the aggregation phenomena also allows to control the distance between the HOMO orbital of the dye and the TiO<sub>2</sub> surface and thereby the electron injection and recombination dynamics. The control over the formation of molecular aggregates onto the semiconductor nanoparticles still remains a key point to achieve better efficiencies but it is not sufficient to explain the low-incident photon to current conversion efficiency (IPCE) observed for phthalocyanine-based dyes, being the factor concerning energy and geometry of LUMO orbitals the second important limit to be overcome.

To this purpose, it has been recently reported [30] that the use of a substituted zinc phthalocyanine with three pushing *tert*-butyl groups and two pulling carboxylic acid groups, results in a sensitizer that exhibits an IPCE of 75%. The cell sensitised with this compound gives a short-circuit photocurrent density of  $(6.50 \pm 0.20) \text{ mA cm}^{-2}$ , an open-circuit voltage of  $(635 \pm 30) \text{ mV}$ , and a fill factor of  $0.74 \pm 0.03$ , which corresponds to an overall conversion efficiency of 3.05%. The presence of such substituents minimizes the aggregation process, increases the solubility in organic solvents, and, owing to their push-pull character, induces directionality in the excited state of the zinc phthalocyanine. Nazeruddin, Cid et al. [31] further extended this “push-pull” idea, presenting a novel zinc phthalocyanine derivative with the same *tert*-butyl substitution and with the carboxylic group directly linked to the Pc ring inducing directionality in the excited state of the molecule. The efficiency of the corresponding solar cell was  $\eta = 3.5\%$  under standard illumination condition. In the same paper the authors stress the possibility to introduce a secondary dye with a complementary visible spectrum (i.e., J.K.2) to obtain the panchromatic sensitisation of the photoelectrode and enhance the efficiency of the device, as a matter of fact they reached the highest value ( $\eta = 7.08\%$ ) among those measured with each single dye. This result suggests that Pcs can be also considered as good candidates for multiple dye cosensitized solar cells.

For the same aim of reaching a large coverage of the visible spectrum, a supramolecular phthalocyanine-squaraine ensemble has been synthesised and characterised.

It exhibits an optical spectrum corresponding to the sum of the absorption of the single components [32], but the low IPCE measured forces the authors to investigate the relationship of processing—microstructure and photovoltaic response.

The strategy in designing new dyes for DSSCs by combining two or more molecules complementing each other in their spectral features to achieve the desired “full-spectrum solar cells” includes dyads systems: new dyes containing ruthenium phthalocyanine and bipyridyl chromophores have been synthesised [33]. DSSCs fabricated using the phthalocyanine dyads were less efficient, however, on the basis of the number of molecules linked to TiO<sub>2</sub> they appear more efficient in the photocurrent generation. These results indicate that the ability of these molecules to cover TiO<sub>2</sub> surface, related to the molecular size, is another significant feature in their success as sensitizing dyes. Nevertheless, the presence of push-pull groups inserted into macrocycle ring shows its effectiveness in the case of a novel zinc phthalocyanine with an extended  $\pi$ -conjugation [34] resulting in an overall conversion efficiency of 2.35%. More recently O'Regan et al. [35] reported the evidence, for a ruthenium phthalocyanine dye, of voltage reduction occurring at both the TiO<sub>2</sub> and SnO<sub>2</sub> surface, caused by the electron/electrolyte recombination reaction catalyzed by the dye. They warn that this problem could be present in other organic dyes and so they consider necessary to determine the molecular basis of this catalytic process in order to develop design rules to avoid it. Another aspect emphasized by Torres group [36, 37] is the role played by the anchoring group (spacer group): the way in which it affects the electron injection from the photoexcited dye into the nanocrystalline TiO<sub>2</sub> has been shown, the recombination rates have been investigated, and the efficiency of the cells has been measured for different anchoring groups. The outcome presented indicates that the IPCE for phthalocyanine bearing an insulating spacer is as low as 9% whereas for those with a conducting spacer an outstanding 80% IPCE was obtained.

It appears entirely evident, from the above listed results, that phthalocyanine-based dyes give performances distant from those obtained with the ruthenium complexes; nevertheless, thanks to the helpful chemical tailoring achievable through organic synthesis, this class of compounds still appear encouraging as sensitizer dyes.

### 3. Bridged Phthalocyanine-Based Dyes for DSSC: Preliminary Results

The results presented here originate from a project aimed to set up different strategies, mainly through synthetic work, for the achievement of new dyes based on metal macrocycles like phthalocyanine or porphyrins as building-blocks for highly conjugated super chromophores. These oligomers should provide the possibility to link themselves to the TiO<sub>2</sub> surface through a suitable anchoring group axially coordinated to the central metal of the macrocycles. In this way some parameters as light-harvesting property, coupling with the semiconductor CB and recombination processes, would be

affected and a strong influence on the surface aggregation is expected as well. The approach is focused on testing the performances of bridged phthalocyanine systems containing two macrocycles per molecule and in comparing the results with those obtained with the correspondent monomeric forms which are the subject of most of scientific work carried on up to now. Here we report the synthesis, the electrochemical measurements, and the optical investigation of three bridged systems (Figure 2), namely,  $\mu$ -carbide bridged iron phthalocyanine (I), hemisubstituted  $\mu$ -carbide bridged iron phthalocyanine (II), and amphi-substituted  $\mu$ -carbide iron phthalocyanine (III) as sensitizers for nanocrystalline TiO<sub>2</sub>. The testing of compound (I) in a DSSC cell was also performed and preliminary results in terms of efficiency are reported.

**3.1. Experimental.** Iron phthalocyanine was purchased by Aldrich and purified by vacuum sublimation at 400°C. Tetra-*tert*-butyl iron phthalocyanine was synthesized according to an existent procedure [38]. All the solvents were anhydrous and distilled before use. Reactions were monitored by TLC employing a polyester layer coated with 250 mm F<sub>254</sub> silica gel. Purification of compounds was performed by column chromatography using silica gel Carlo Erba Reactifs SDS 60A C.C. 35–70 mm. Infrared spectra were recorded on a Shimadzu IR prestige-21 spectrometer in KBr pellets or in nujol mull. UV-vis spectra were recorded on a Perkin-Elmer Lambda 950 UV-vis. NIR spectrophotometer. Thermal analysis was performed with TA Instrument SDT Q600 simultaneous TGA-DTA-DSSC apparatus.

#### 3.1.1. Synthesis

**Synthesis of  $\mu$ -Carbide Bridged Iron Phthalocyanine: FePc=C=FePc (I).** The  $\mu$ -carbide compound has been prepared and characterised according to the procedure already reported in literature [39]. A mixture of iron phthalocyanine and sodium dithionite was heated 140–145°C in 1-chloronaphthalene then carbon tetraiodide was added, and the solution was stirred for 40 minutes. After cooling, the reaction mixture was filtered, and the solid residue washed with acetone, distilled water, and acetone again and then dried to constant weight under vacuum. The crude product was dissolved in N-methylimidazole (1-Meim) and the resulting [(1-Meim)(FePc)]<sub>2</sub>C was recrystallized from 1:1 hexane/acetone. The crystalline compound was then treated at 250° for 30 minutes to remove N-methylimidazole and obtain the desired molecule. Elemental analysis, visible, infrared, and NMR spectra were performed to check the purity of the product.

**Synthesis of Hemisubstituted  $\mu$ -Carbide Bridged Iron: (t-bu)<sub>4</sub>PcFe=C=FePc (II).** The procedure followed is similar to the previous one: 86 mg (0.15 mmol) of iron phthalocyanine and 120 mg (0.15 mmol) of tetra-*tert*-butyl iron phthalocyanine were dissolved in xylene (7 ml) with 303 mg (1.7 mmol) of sodium dithionite. The mixture was then heated to reflux and then 312 mg (0.60 mmol) of

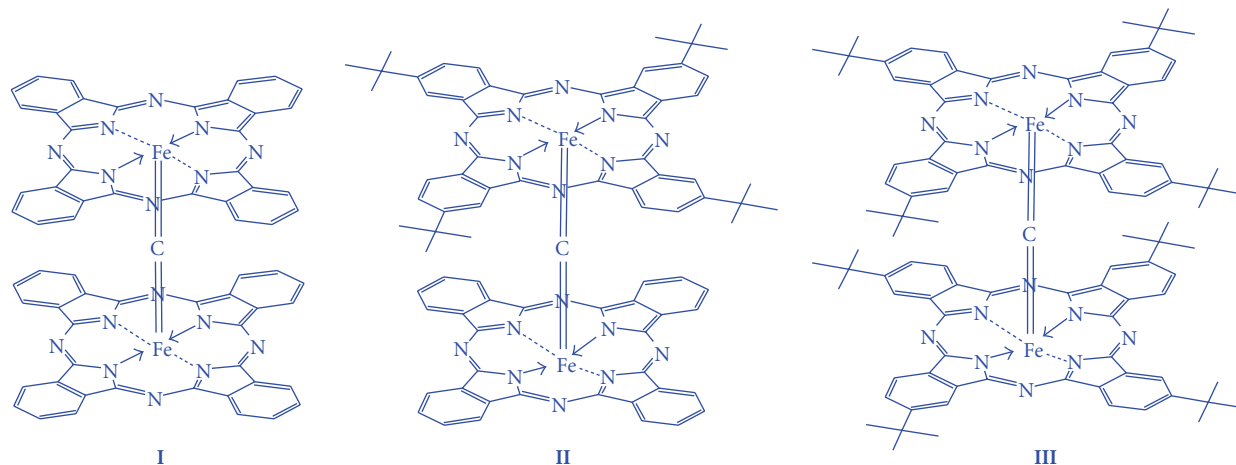


FIGURE 2:  $\mu$ -carbide bridged iron phthalocyanine (I), hemisubstituted  $\mu$ -carbide bridged iron phthalocyanine (II), and amphi-substituted  $\mu$ -carbide iron phthalocyanine (III).

$\text{Cl}_4$  were added. After 45 minutes it was cooled to room temperature, diluted with diethyl ether, washed with water and  $\text{Na}_2\text{S}_2\text{O}_3$  (saturated solution), dried over sodium sulphate, and concentrated under reduced pressure. The crude product, consisting of three species, was then purified with column chromatography on silica gel using 10:1 and 9:1 petroleum ether/dioxane as mobile phase.

*Synthesis of Amphi-Substituted  $\mu$ -Carbide Bridged Iron Phthalocyanine:  $(t\text{-bu})_4\text{PcFe}=\text{C}=\text{FePc}(t\text{-bu})_4$  (III).* 150 mg (0.19 mmol) of tetra-tert-butyl iron phthalocyanine were dissolved in 5 ml of xylene with 190 mg (1.1 mmol) of sodium dithionite. The mixture was heated to reflux in an oil bath and then 195 mg (0.37 mmol) of  $\text{Cl}_4$  were added. After 45 minutes the solution was cooled, diluted with diethyl ether, washed with water and with a saturated solution of  $\text{Na}_2\text{S}_2\text{O}_3$ , dried over sodium sulphate, and concentrated under reduced pressure. The crude product was then purified by column chromatography on silica gel using a mixture of petroleum ether and dioxane (9:1) as mobile phase. The compound is soluble in the most common organic solvents, such as dichloromethane, chloroform, ethanol, and THF.

*General Procedure for the Adducts Formation with Isonicotinic Acid (IsA).* 1 equivalent of (I), (II) or (III) was dissolved in a few ml. of THF and stirred at room temperature, then 2 equivalent of isonicotinic acid were added and the mixture was stirred for one, two, or three days, depending on the chosen bridged system. Then, for the unsubstituted  $(\text{FePc})_2\text{C}$  the solution was centrifuged, the solid residue was washed several times with  $\text{H}_2\text{O}/\text{MeOH}$  1:1 to remove the excess of isonicotinic acid, and then dried under vacuum. In the other cases the mixture was first concentrated under reduced pressure and then washed as previously described. Thermogravimetric analysis showed that two molecules of IsA were lost in one step with a loss of weight of 14.0%, ( $T = 180 - 210^\circ\text{C}$ ) being the theoretical value of 13.3%.

*3.1.2. Spectroscopic Study.* Time resolved fluorescence measurements were carried out by a time-correlated-single-photon-counting (TCSPC) [40] homemade apparatus ( $\lambda_{\text{ex}} = 575\text{ nm}$ ), which has been already described in [41]. The fluorescence decay profiles were analysed through a nonlinear least-squares iterative deconvolution procedure based on the Marquardt algorithm [42] achieving an instrumental resolution of about few tens of picoseconds. The total fluorescence decay curves were fitted to a multiexponential decay equation [43]:  $I(t) = I_0 \sum \alpha_i \exp(-t/\tau_i)$ , where  $I(t)$  is the total fluorescence decay curve,  $I_0$  is the intensity at  $t = 0$ , and  $\alpha_i$  and  $\tau_i$  are relative amplitude and lifetime of  $i$ th component (the normalization condition being  $\sum_i \alpha'_i = 1$ ), respectively.

*3.1.3. Electrochemical Measurements.* Cyclic voltammograms were recorded at  $25^\circ\text{C}$  with a computer-aided system (AMEL INSTRUMENTS 2059 potentiostat/galvanostat, 568 function generator) in a conventional three-electrode cell; a platinum disk was used as working electrode together with a platinum wire as auxiliary electrode. The reference electrode was  $\text{Ag}/\text{AgNO}_3$  (0.01 M) in distilled acetonitrile ( $E_0$  versus SCE = 0.298 V). The samples solutions were  $10^{-4}\text{ M}$  in distilled anhydrous dichloromethane, and tetra(*n*-butyl)ammonium tetrafluoroborate (TBATFB, 0.1 M) was used as supporting electrolyte. The solutions were previously purged for 10 minutes with nitrogen and all measurements were performed in inert atmosphere. Because the solubility of some of these compounds in  $\text{CH}_2\text{Cl}_2$  was poor, we added 1-Meim as coordinating base when needed.

*3.1.4. DSSC Fabrication.*  $0.25\text{ cm}^2$   $\text{TiO}_2$  (P25-Degussa) active area was deposited onto FTO conducting glass through "doctor-blade" technique,  $\text{TiO}_2$  layer was sintered at  $450^\circ\text{C}$  for 45 minutes, then kept at  $80^\circ\text{C}$  within 3 hours and immediately used for the dipping process (averaged thickness 16–18  $\mu\text{m}$ ). A 0.5 mM solution of  $(\text{IsAFcPc})_2\text{C}$  in THF was freshly prepared and used to sensitize the  $\text{TiO}_2$  layer and

no coadsorbents or antiaggregation agents such as CHENO (deoxycholic acids) were used. Dipping time was 14 hours (during night) at room temperature; after that the photoanode was rinsed with THF. A sandwich cell was prepared using the dye anchored TiO<sub>2</sub> film as working electrode and a second conducting glass, coated with chemically deposited platinum (PT-1 platinum paste purchased from Dyesol) as photocathode. The two electrodes were superimposed with a thin transparent film of Surlyn polymer gasket (25 μm) and the device was sealed by heating. The internal space was filled with HSE electrolyte (purchased by Dyesol) by using a vacuum backfilling system. The electrolyte-injecting hole on the counter electrode glass substrate was sealed with a Surlyn sheet and a thin glass cover by heating.

## 4. Results and Discussion

**4.1. Spectroscopic Properties.** The UV/Vis spectra of the compounds (I–III) in solution exhibit the feature typical of phthalocyanine complexes (Figure 3) with an intense band in the range of 550–750 nm (Q band). As expected the *ter*-butyl substitution moves the maximum of the absorption peak from 620 nm (unsubstituted bridge) to 637 nm (substitution on both macrocycles) for the increasing number of pushing groups on the peripheral rings. A similar trend was observed in the fluorescence spectra as well as shown in Table 1. As far as concern of the IR spectra, it is worthy to point out that in all the cases a strong band between 997 and 1007 cm<sup>-1</sup>, already attributed to the Fe=C=Fe stretching was observed [38]. In the hemisubstituted compound [(*t*-bu)<sub>4</sub>PcFe=C=FePc] this band is split likely owing to the different strength constants of the two parts of the bridged system. In addition, the presence of four or eight *ter*-butyl groups is well shown in the aliphatic C–H stretching region (2950 cm<sup>-1</sup>) while a gradual decreasing of intensity of phenyl C–H stretching in the range 1600–700 cm<sup>-1</sup> is observed going from compound (I) to (III).

**4.2. Emission Measurements.** The photo properties of the unsubstituted bridged system (I) have been investigated in dichloromethane, and the steady-state fluorescence emission spectrum ( $\lambda_{\text{ex}} = 620$  nm) is shown in Figure 4. A rather broad absorption with maximum centred around 650 nm can be observed, while in the inset its excitation spectrum ( $\lambda_{\text{em}} = 680$  nm) presents an intense band at 620–625 nm attributable to the  $\pi$ - $\pi^*$  transition of the compound (Q band).

Fluorescence emission decays of the adduct (IsAFePc)<sub>2</sub>C in THF ( $\lambda_{\text{em}} = 650$  nm) exhibits a biexponential behaviour with two contributions (Figure 5); the first corresponding to 82% of amplitude has a life time of 0.9 ns and the second one (18%) has a life time of 8.2 ns. We suggest that the more accelerated decay, which is prevalent, is attributable to the  $\mu$ -carbide bridge while the slower can be assigned to a monomeric species often present as impurity. Time resolved emission measurements of (IsAFePc)<sub>2</sub>C sensitised TiO<sub>2</sub> show a very efficient quenching with a life time of 0.3 ns ( $a = 98\%$ ). This appreciable reduction of the

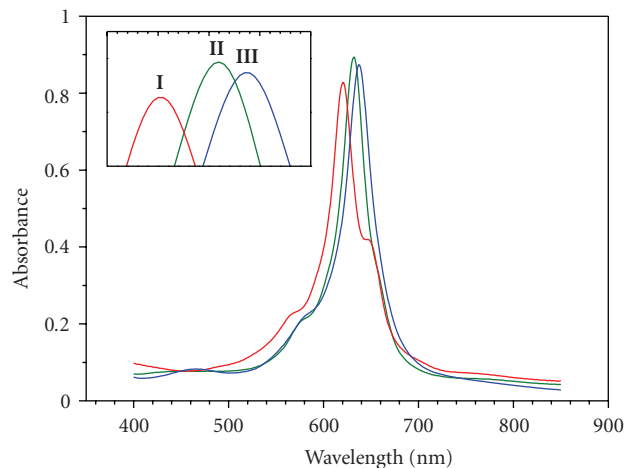


FIGURE 3: Visible spectra of compounds I, II, and III.

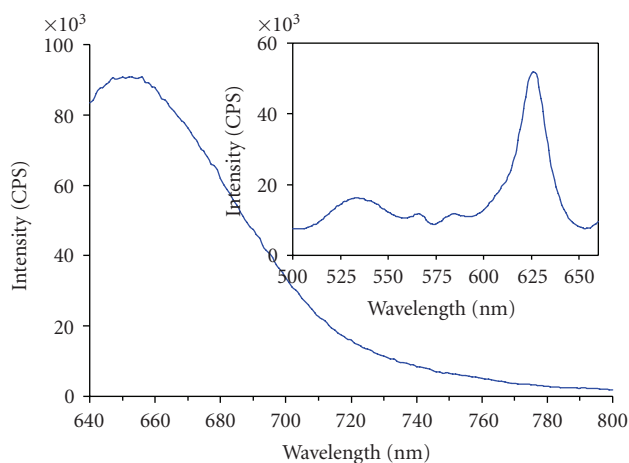


FIGURE 4: Steady-state fluorescence emission spectrum ( $\lambda_{\text{ex}} = 620$  nm) and (inset) corresponding excitation spectrum ( $\lambda_{\text{em}} = 680$  nm) of compound (I).

fluorescence life time (from 0.9 to 0.3 ns) is, in principle, indicative of an efficient electron injection occurring at the interface, likely due to electron injection from the singlet excited state of the molecule into the conduction band of the TiO<sub>2</sub>. Semiquantitative estimation of time scale of this latter phenomenon can be performed taking into account that  $\tau \propto 1/\Sigma k_i$  ( $k =$  kinetic constant of  $i$ th process of excited state deactivation): in our case the measured fluorescence lifetime of the dye goes from 0.9 ns to 0.3 ns in solution and TiO<sub>2</sub>, respectively, and the kinetic of electron injection process would be estimated to occur at  $\approx 0.45$  ns<sup>-1</sup>. This value can be considered fast enough in relation to the lifetime of the compound in solution and it is in the same order of magnitude of that one measured for several monomeric phthalocyanines [35].

**4.3. Electrochemical Measurements.** To assign the electric potential of the HOMO orbitals of these bridged systems, we investigated their electrochemical properties in the anodic

TABLE 1: Experimental Spectral and Electrochemical data of **I–III** dyes.

dye	Abs <sub>max</sub> <sup>a</sup> [nm]	Em <sub>max</sub> <sup>a</sup> [nm]	E <sub>(S<sup>+/S</sup>)</sub> <sup>b</sup> [V] versus SCE	E <sub>(0-0)</sub> <sup>c</sup> [V] (Abs/Em)	E <sub>(S<sup>+/S*</sup>)</sub> <sup>d</sup> [V] versus SCE
( <b>I</b> ) + 1-Methylimidazole	621	696	0.434	1.88	-1.45
( <b>II</b> )	632	702	0.419	1.86	-1.44
( <b>II</b> ) + 1-Methylimidazole	620	702	0.328	1.87	-1.54
( <b>III</b> )	637	702	0.387	1.86	-1.47
( <b>III</b> ) + 1-Methylimidazole	627	702	0.383	1.86	-1.48

<sup>a</sup>Absorption and emission spectra in CH<sub>2</sub>Cl<sub>2</sub> solution. <sup>b</sup>Ground state oxidation potential versus SCE. <sup>c</sup>0-0 transition energy estimated from the intercept of the normalized absorption and emission spectra. <sup>d</sup>Estimated LUMO energies from the estimated HOMO energies (ground state oxidation potential) and the 0-0 transition energies.

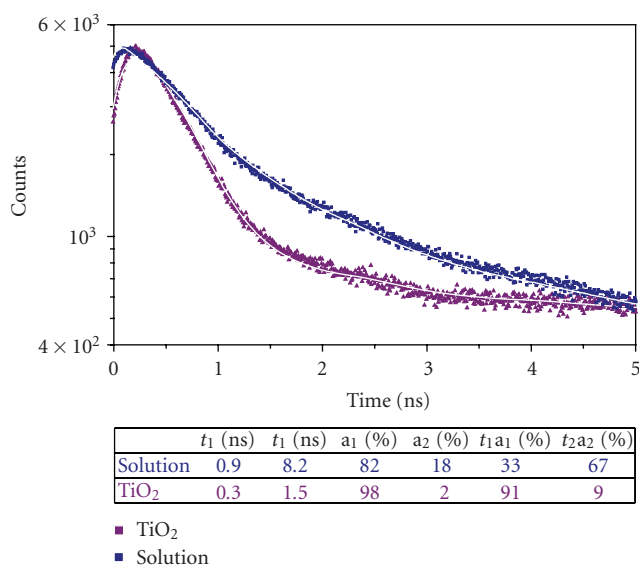


FIGURE 5: Experimental (dot) and calculated (line) fluorescence emission decays of (IsAFcPc)<sub>2</sub>C ( $\lambda_{em} = 650$  nm), in solution and on TiO<sub>2</sub> substrate; at the bottom table of fitting results;  $\tau$ : life-time,  $a$ : amplitude.

range with cyclic voltammetry, allowing the electrochemical characterization to assess the energetic position of frontier orbital HOMO by the ground-state excitation potential  $E_{(S^+/S)}$  of the first oxidation process. In Table 1 are summarised the first oxidation potentials of the **I**, **II**, and **III** compounds together with their correspondent spectral data and LUMO calculated energy levels.

Because the solubility of unsubstituted compound **I** was very low it has been possible to carry on the electrochemical measurements only on the corresponding more soluble 1-methylimidazole bis-adduct, while substituted compounds **II** and **III**, considerably more soluble, have been tested both in adducted form and not. The electrochemical behaviour of the  $\mu$ -carbido iron complex (**I**) has been already investigated in the past both for phthalocyanine and porphyrin systems [44, 45]. In general, two oxidations and two reductions are expected for these systems being all processes centred on the macrocycles: the central metal iron is in a high-oxidation state (IV) and it does not undertake further oxidative processes. The oxidation potentials are specific to

the ligand-directed singly and doubly oxidized complex and there is a distinct separation of the half-wave potential in the successive ring oxidations. Due to the strong excitonic interactions of the closely adjacent Pc ligands in such diphthalocyanine compounds, the first macrocycle is oxidized more easily while the second one requests higher potentials. Furthermore, it is well known [45] that the first oxidation potential of nonmonomeric phthalocyanine derivatives is  $\sim 0.3$  V (versus SCE), lower than the analogous potential of monomeric species which show ring-centred redox process, because of the delocalization of the positive charge over the whole system. Also, axial ligation with azo-bases and peripheral substitution with electron-releasing groups are known to affect the first oxidation potential because of the above mentioned effect, even if it is not predictable which of the two effects is more meaningful. In presence of 1-N-methylimidazole our experimental results on (**I**) are in total accord with what is published by Lancon and Kadish. [45] and the general trend is consistent being the first oxidation potential of the compound (**I**) > (**III**), due to the presence of *ter*-butyl groups that have a further stabilizing effect on the monooxidized complex. An apparent anomalous value, always in the presence of N-base, has been found for the system (**II**) that shows the lowest oxidation potential value; in this system we have only one ring replaced with *ter*-butyl groups and we think that in this specific case the addition of the N-base coordinated to the metal central and the presence of pushing groups lead to the observed lowest value. In fact, if we compare the first oxidation potential values of (**II**) and (**III**) measured in absence of N-base, being the stabilizing effect exclusively determined by the presence of the pushing groups, the situation is reversed and as expected the first oxidation potential is lower when in both rings are inserted pushing groups.

The electrochemical data have allowed the assessment of the ground state potentials ( $S^+/S$ ) of the species (**I**)–(**III**) and this data together with the correspondent 0-0 transition energies, estimated from the intercept of absorption and emission spectra, give the energy levels of the singlet excited state (LUMO) of the compounds according to the equation:  $E_{(S^+/S^*)} = E_{(S^+/S)} - E_{(0-0)}$ . In Table 1 are summarised all the relevant absorption/emission values and the calculated HOMO/LUMO energy levels for all the sensitizers.

The main observation is that the inserted pushing groups do not affect strongly the energy level position of LUMO

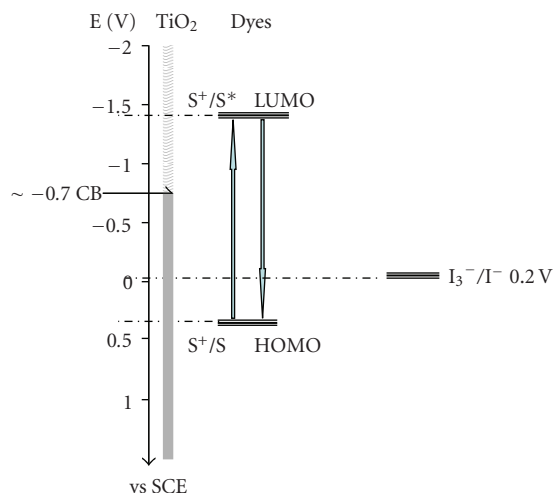


FIGURE 6: Energy level diagram from spectral and electrochemical data.

orbital and if we sketch the energy level diagram of the three compounds in comparison to the  $\text{TiO}_2$  conduction band and the redox couple  $\text{I}^-/\text{I}_3^-$  (Figure 6) some significant remarks can be done. In principle we can say that one of the fundamental requisites have been satisfied: the LUMO position of the compounds ( $-1.44$ ;  $-1.54$ ) is widely more negative than the  $\text{TiO}_2$  conduction band ( $-0.74$  V versus SCE); therefore all compounds should have sufficient driving force for electron injection to the semiconductor. Nevertheless it is well known that this is a necessary but not sufficient condition. In fact to have a good overlap between the LUMO orbital and the  $\text{TiO}_2$  conduction band, the excited states must possess directionality and also the kinetic of the process must be favourable. Furthermore, the HOMO levels of the dyes are lower than the energy level of the redox couple  $\text{I}^-/\text{I}_3^-$  ( $0.2$  V versus SCE) enabling the dye regeneration reactions. The difference between the two levels appears more favourable for the compound (I) (circa  $200$  mV) while for compounds (II) and (III) this difference has so low values that the process of the dye regeneration from the couple  $\text{I}^-/\text{I}_3^-$  can seriously be called into question. Being well known that the efficiency of a cell depends on the balance between the electron injection into the conduction band and the back transfer of injected electrons from conduction band of  $\text{TiO}_2$  towards the dye cation radical, we should ensure that there is enough driving force for the regeneration reaction in order to avoid the recapture by the dye cation or at least to make this process as slow as possible.

**4.4. DSSC Device Performance.** Dye sensitized solar cells with  $\text{TiO}_2$  layer covered by  $(\text{IsAFcPc})_2\text{C}$  present average  $V_{oc}$  and  $J_{sc}$  values in the range of hundred millivolt and microampere, respectively; to be more precise the best cell values (Figure 7) are  $V_{oc} = 359$  mV,  $J_{sc} = 305 \mu\text{A}/\text{cm}^2$ , and  $\text{FF} = 62.9\%$  and an efficiency of  $0.07\%$ . It is important to note that the cells reach these values after a quite long stabilizing period (see Table 2) during which it is possible to note a slow colour change of the electrolyte solution, from yellow to green,

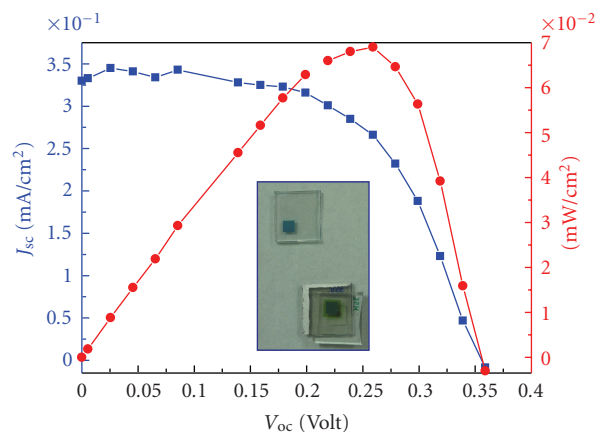


FIGURE 7: J/V plot of DSSC cell with compound (I) after 3 weeks; in the inset: picture of the cell as done (blue) and after 3 weeks.

TABLE 2: Performances of the same DSSC cell during time.

Measurements	Delay Time	$J_{sc}$ ( $\mu\text{A}/\text{cm}^2$ )	$V_{oc}$ (mV)	FF (%)	$\eta$ (%)
(a)	24 hours	181	275	36.1	0.018
(b)	1 week	227	276	41.1	0.026
(c)	2 week	252	326	48.9	0.040
(d)	3 week	305	359	62.9	0.069

and similar effect is also visible for the sensitized  $\text{TiO}_2$ , changing from deep blue to green (Figure 7 inset). This effect can be ascribable to the electrolyte system: it is known that different benzimidazole derivatives [46] are used as additives in the electrolyte solution and these compounds can coordinate the iron atom displacing the isonicotinic acid. Similar behaviour is expected if *ter*-butyl pyridine would be used [47].

Taking into account the molecular symmetry, this phenomenon can have a double effect: (1) benzimidazole derivative (that only for convenience is represented as *N*-methyl-benzimidazole) can remove the dye from the titanium layer displacing the isonicotinic acid directly bound to the  $\text{TiO}_2$  surface; as direct consequence of that it is possible to note the electrolyte solution becomes green; (2) benzimidazole compound can alternatively substitute the  $\text{TiO}_2$ -nonbound isonicotinic acid, inducing a general asymmetry in the molecule and, acting as pushing electron donating group, it can increase or create an axially aligned dipole moment which can improve the molecular performances (Figure 8). Considering the overall result observed during time (increased  $J_{sc}$  and  $V_{oc}$ ) it is possible to confirm that the displacement of  $\text{TiO}_2$ -nonbound isonicotinic acid is the main effect on the cell performance. These measurements underline how the design of new dyes has to be planned taking into account the whole system and how the electrolyte solution has to be tailored as a function of the physical-chemical properties of the dye.

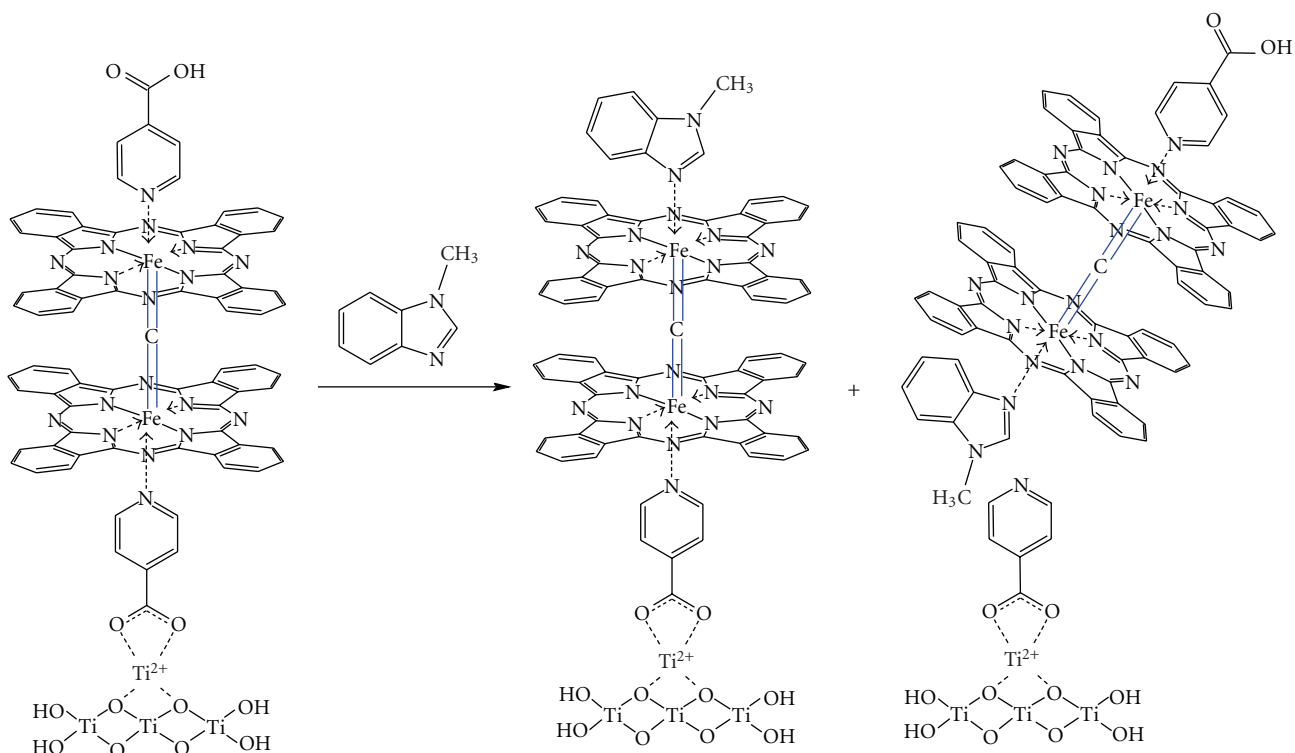


FIGURE 8: Hypothesis on interaction of benzoimidazole derivatives on the bonding of the dye over the  $\text{TiO}_2$  substrate.

## 5. Conclusion

**5.1. Conclusions.** In this work we have presented the synthesis and characterization of new dyes for DSSC cells in the attempt of exploiting the behaviour of dimeric phthalocyanine systems in comparison with their monomeric forms widely investigated during the last years. Although only compound (**I**) has been tested in a DSSC cell and, in terms of efficiency, the obtained results are not so satisfactory, we want to point out some remarks: all compounds can be anchored to  $\text{TiO}_2$  semiconductor without the presence of any anti-aggregation molecules, confirming that for such phthalocyanine systems the anchoring procedure to the semiconductor through the axial position prevents aggregation phenomena. As shown by time-resolved fluorescence measurements we observed a significant emission quenching attributable to an electron transfer from the dye to the semiconductor substrate with a sub-nanosecond kinetic process. In spite of that, we measured a poor efficiency very likely ascribed to different factors: (a) the probable replacement of isonicotinic acid by benzoimidazole derivative, and (b) the too low ionisation potential of the dye that makes difficult its regeneration by the  $\text{I}^-/\text{I}_3^-$  couple and the formation of a complex between the cation species and the  $\text{I}_3^-$  anion would be favoured. Taking into account all these considerations, it is not wrong to think that the performances of the cell could be considerably improved changing some elements in the cell construction up to redox shuttle and additives; it is well accepted that changing one of the greatest elements in a cell requires at least a simultaneous change/optimisation of

all other elements. Further experimental works to reach this purpose are under current investigation.

## Acknowledgments

The authors and in particular G. Zanotti thank the project CHOSE (Centre for Hybrid and Organic Solar Energy) of Regione "Lazio" for supporting this paper. Many thanks also go to Francesco Ghetti (IBF-CNR, Pisa) for preliminary time-resolved measurements and Norberto Micali (IPCF-CNR, Messina) for making available the apparatus for definitive time-resolved fluorescence measurements. The authors are very grateful to Paolo Plescia (ISMN-CNR, Roma) for thermogravimetric analysis.

## References

- [1] N. S. Lewis, "Powering the planet," *MRS Bulletin*, vol. 32, no. 10, pp. 808–820, 2007.
- [2] M. Grätzel, "Photoelectrochemical cells," *Nature*, vol. 414, no. 6861, pp. 338–344, 2001.
- [3] M. Grätzel, "Dye-sensitized solar cells," *Journal of Photochemistry and Photobiology C*, vol. 4, no. 2, pp. 145–153, 2003.
- [4] M. K. Nazeeruddin, A. Kay, I. Rodicio et al., "Conversion of light to electricity by cis- $\text{X}_2$ Bis(2,2'-bipyridyl-4,4'-dicarboxylate)ruthenium(II). Charge-transfer sensitizers ( $\text{X} = \text{Cl}^-$ ,  $\text{Br}^-$ ,  $\text{I}^-$ ,  $\text{CN}^-$ , and  $\text{SCN}^-$ ) on nanocrystalline  $\text{TiO}_2$  electrodes," *Journal of the American Chemical Society*, vol. 115, no. 14, pp. 6382–6390, 1993.

- [5] Y. Tachibana, J. E. Moser, M. Grätzel, D. R. Klug, and J. R. Durrant, "Subpicosecond interfacial charge separation in dye-sensitized nanocrystalline titanium dioxide films," *Journal of Physical Chemistry*, vol. 100, no. 51, pp. 20056–20062, 1996.
- [6] T. W. Hamann, R. A. Jensen, A. B. F. Martinson, H. V. Ryswyk, and J. T. Hupp, "Advancing beyond current generation dye-sensitized solar cells," *Energy & Environmental Science*, vol. 1, no. 1, pp. 66–78, 2008.
- [7] A. Mishra, M. K. R. Fischer, and P. Bäuerle, "Metal-free organic dyes for dye-sensitized solar cells: from structure: property relationships to design rules," *Angewandte Chemie*, vol. 48, no. 14, pp. 2474–2499, 2009.
- [8] H. Tian and F. Meng, "Solar cells based on nanoporous titania films filled with conjugated polymers," in *Organic Photovoltaics: Mechanisms, Materials, and Devices*, S. S. Sun and N. S. Sariciftci, Eds., p. 313, CRC, London, UK, 2005.
- [9] H. Tian, X. Yang, R. Chen, A. Hagfeldt, and L. Sun, "A metal-free "black dye" for panchromatic dye-sensitized solar cells," *Energy & Environmental Science*, vol. 2, no. 6, pp. 674–677, 2009.
- [10] D. P. Hagberg, J.-H. Yum, H. Lee et al., "Molecular engineering of organic sensitizers for dye-sensitized solar cell applications," *Journal of the American Chemical Society*, vol. 130, no. 19, pp. 6259–6266, 2008.
- [11] S. Ito, S. M. Zakeeruddin, R. Humphry-Baker et al., "High-efficiency organic-dye-sensitized solar cells controlled by nanocrystalline-TiO<sub>2</sub> electrode thickness," *Advanced Materials*, vol. 18, no. 9, pp. 1202–1205, 2006.
- [12] K. Hara, K. Sayama, Y. Ohga, A. Shinpo, S. Suga, and H. Arakawa, "A coumarin-derivative dye sensitized nanocrystalline TiO<sub>2</sub> solar cell having a high solar-energy conversion efficiency up to 5.6%," *Chemical Communications*, no. 6, pp. 569–570, 2001.
- [13] K. Hara, M. Kurashige, Y. Dan-oh et al., "Design of new coumarin dyes having thiophene moieties for highly efficient organic-dye-sensitized solar cells," *New Journal of Chemistry*, vol. 27, no. 5, pp. 783–785, 2003.
- [14] G. Calogero, G. Di Marco, S. Cazzanti, et al., "Efficient dye-sensitized solar cells using red turnip and purple wild Sicilian prickly pear fruits," *International Journal of Molecular Sciences*, vol. 11, no. 1, pp. 254–267, 2010.
- [15] C. G. Claessens, U. Hahn, and T. Torres, "Phthalocyanines: from outstanding electronic properties to emerging applications," *The Chemical Record*, vol. 8, no. 2, pp. 75–97, 2008.
- [16] C. Leznoff and A. B. P. Lever, Eds., *Phthalocyanines: Properties and Applications*, vol. 1–4, Wiley-VCH, Cambridge, UK, 1989.
- [17] G. De La Torre, C. G. Claessens, and T. Torres, "Phthalocyanines: old dyes, new materials. Putting color in nanotechnology," *Chemical Communications*, no. 20, pp. 2000–2015, 2007.
- [18] H. Imahori, T. Umeyama, and S. Ito, "Large  $\pi$ -aromatic molecules as potential sensitizers for highly efficient dye-sensitized solar cells," *Accounts of Chemical Research*, vol. 42, no. 11, pp. 1809–1818, 2009.
- [19] Y. Ooyama and Y. Harima, "Molecular designs and syntheses of organic dyes for dye-sensitized solar cells," *European Journal of Organic Chemistry*, no. 18, pp. 2903–2934, 2009.
- [20] B. E. Hardin, E. T. Hoke, P. B. Armstrong et al., "Increased light harvesting in dye-sensitized solar cells with energy relay dyes," *Nature Photonics*, vol. 3, no. 7, pp. 406–411, 2009.
- [21] K. Lee, S. W. Park, M. J. Ko, K. Kim, and N.-G. Park, "Selective positioning of organic dyes in a mesoporous inorganic oxide film," *Nature Materials*, vol. 8, no. 8, pp. 665–671, 2009.
- [22] J. He, G. Benko, F. Korodi et al., "Modified phthalocyanines for efficient near-IR sensitization of nanostructured TiO<sub>2</sub> electrode," *Journal of the American Chemical Society*, vol. 124, no. 17, pp. 4922–4932, 2002.
- [23] M. D. K. Nazeeruddin, R. Humphry-Baker, M. Grätzel, and B. A. Murrer, "Efficient near IR sensitization of nanocrystalline TiO<sub>2</sub> films by ruthenium phthalocyanines," *Chemical Communications*, no. 6, pp. 719–720, 1998.
- [24] E. Palomares, M. V. Martínez-Díaz, S. A. Haque, T. Torres, and J. R. Durrant, "State selective electron injection in non-aggregated titanium phthalocyanine sensitized nanocrystalline TiO<sub>2</sub> films," *Chemical Communications*, vol. 10, no. 18, pp. 2112–2113, 2004.
- [25] A. Morandeira, I. Lopez-Duarte, M. V. Martinez-Diaz et al., "Slow electron injection on Ru-phthalocyanine sensitized TiO<sub>2</sub>," *Journal of the American Chemical Society*, vol. 129, no. 30, pp. 9250–9251, 2007.
- [26] J. He, A. Hagfeldt, S.-E. Lindquist et al., "Phthalocyanine-sensitized nanostructured TiO<sub>2</sub> electrodes prepared by a novel anchoring method," *Langmuir*, vol. 17, no. 9, pp. 2743–2747, 2001.
- [27] S. Eu, T. Katoh, T. Umeyama, Y. Matano, and H. Imahori, "Synthesis of sterically hindered phthalocyanines and their applications to dye-sensitized solar cells," *Dalton Transactions*, no. 40, pp. 5476–5483, 2008.
- [28] J.-H. Yum, S.-R. Jang, R. Humphry-Baker et al., "Effect of coadsorbent on the photovoltaic performance of zinc phthalocyanine-sensitized solar cells," *Langmuir*, vol. 24, no. 10, pp. 5636–5640, 2008.
- [29] A. Morandeira, I. López-Duarte, B. O'Regan, et al., "Ru(II)-phthalocyanine sensitized solar cells: the influence of co-adsorbents upon interfacial electron transfer kinetics," *Journal of Materials Chemistry*, vol. 19, no. 28, pp. 5016–5026, 2009.
- [30] P. Y. Reddy, L. Giribabu, C. Lyness et al., "Efficient sensitization of nanocrystalline TiO<sub>2</sub> films by a near-IR-absorbing unsymmetrical zinc phthalocyanine," *Angewandte Chemie*, vol. 46, no. 3, pp. 373–376, 2007.
- [31] J.-J. Cid, J.-H. Yum, S.-R. Jang et al., "Molecular cosensitization for efficient panchromatic dye-sensitized solar cells," *Angewandte Chemie*, vol. 46, no. 44, pp. 8358–8362, 2007.
- [32] F. Silvestri, I. Lopez-Duarte, W. Seitz et al., "A squaraine-phthalocyanine ensemble: towards molecular panchromatic sensitizers in solar cells," *Chemical Communications*, no. 30, pp. 4500–4502, 2009.
- [33] T. Rawling, C. Austin, F. Buchholz, S. B. Colbran, and A. M. McDonagh, "Ruthenium phthalocyanine-bipyridyl dyads as sensitizers for dye-sensitized solar cells: dye coverage versus molecular efficiency," *Inorganic Chemistry*, vol. 48, no. 7, pp. 3215–3227, 2009.
- [34] L. Giribabu, C. V. Kumar, P. Y. Reddy, J.-H. Yum, M. Grätzel, and M. K. Nazeeruddin, "Unsymmetrical extended  $\pi$ -conjugated zinc phthalocyanine for sensitization of nanocrystalline TiO<sub>2</sub> films," *Journal of Chemical Sciences*, vol. 121, no. 1, pp. 75–82, 2009.
- [35] B. C. O'Regan, I. López-Duarte, M. V. Martínez-Díaz et al., "Catalysis of recombination and its limitation on open circuit voltage for dye sensitized photovoltaic cells using phthalocyanine dyes," *Journal of the American Chemical Society*, vol. 130, no. 10, pp. 2906–2907, 2008.
- [36] J.-J. Cid, M. García-Iglesias, J.-H. Yum, et al., "Structure-function relationships in unsymmetrical zinc phthalocyanines for dye-sensitized solar cells," *Chemistry - A European Journal*, vol. 15, no. 20, pp. 5130–5137, 2009.

- [37] F. Silvestri, M. García-Iglesias, J. Yumb, et al., "Carboxy-1,4-phenylenevinylene- and carboxy-2,6-naphthylene-vinylene unsymmetrical substituted zinc phthalocyanines for dye-sensitized solar cells," *Journal of Porphyrins and Phthalocyanines*, vol. 13, no. 3, pp. 369–375, 2009.
- [38] J. Metz, O. Schneider, and M. Hanack, "Synthesis and properties of substituted (phthalocyaninato)iron and -cobalt compounds and their pyridine adducts," *Inorganic Chemistry*, vol. 23, no. 8, pp. 1065–1071, 1984.
- [39] G. Rossi, V. L. Goedken, and C. Ercolani, " $\mu$ -carbido-bridged iron phthalocyanine dimers: synthesis and characterization," *Journal of the Chemical Society, Chemical Communications*, no. 1, pp. 46–47, 1988.
- [40] D.V. O'Connor and D. Phillips, *Time-Correlated Single Photon Counting*, Academic Press, New York, NY, USA, 1981.
- [41] N. Angelini, N. Micali, V. Villari, P. Mineo, D. Vitalini, and E. Scamporrino, "Interactions between water soluble porphyrin-based star polymer and amino acids: spectroscopic evidence of molecular binding," *Physical Review E*, vol. 71, no. 2, Article ID 021915, 7 pages, 2005.
- [42] D.W. Marquadt, "An algorithm for least-squares estimation of nonlinear parameters," *Journal of the Society for Industrial and Applied Mathematics*, vol. 11, no. 2, pp. 431–441, 1963.
- [43] J. R. Lakowicz, *Principles of Fluorescence Spectroscopy*, Kluwer Academic/Plenum Publishers, New York, NY, USA, 1999.
- [44] A. Kienast, L. Galich, K. S. Murray et al., " $\mu$ -carbido diporphyrinates and diphthalocyaninates of iron and ruthenium," *Journal of Porphyrins and Phthalocyanines*, vol. 1, no. 2, pp. 141–157, 1997.
- [45] D. Lancon and K. M. Kadish, "Electrochemistry of the  $\mu$ -carbido iron tetraphenylporphyrin dimer, ((TPP)Fe)<sub>2</sub>C, in nonaqueous media. Evidence for axial ligation by pyridine," *Inorganic Chemistry*, vol. 23, no. 24, pp. 3942–3947, 1984.
- [46] H. Choi, I. Raabe, D. Kim, et al., "High molar extinction coefficient organic sensitizers for efficient dye-sensitized solar cells," *Chemistry - A European Journal*, vol. 16, no. 4, pp. 1193–1201, 2010.
- [47] M. K. Nazeeruddin, F. De Angelis, S. Fantacci et al., "Combined experimental and DFT-TDDFT computational study of photoelectrochemical cell ruthenium sensitizers," *Journal of the American Chemical Society*, vol. 127, no. 48, pp. 16835–16847, 2005.



**Hindawi**

Submit your manuscripts at  
<http://www.hindawi.com>

